Inorg. Chem. **2002**, *41*, 5912–5919

Acid–Base Equilibrium of Aqua–Chromium–Dioxolene Complexes Aimed at Formation of Oxo–Chromium Complexes

Kazushi Shiren and Koji Tanaka*

Institute for Molecular Science and CREST, Japan Science and Technology Corporation (JST), 38 Nishigonaka, Myodaiji, Okazaki, Aichi 444-8585, Japan

Received May 1, 2002

A series of aqua–Cr(III)–dioxolene complexes, $[Cr(OH_2)(3,5\text{-}Bu_2SQ)(trpy)](ClO_4)_2$ (**1s**), $[Cr(OH_2)(3,5\text{-}Bu_2Cat)(trpy)]ClO_4$ (**1c**), $[Cr(OH_2)(3,6\text{-}Bu_2SQ)(trpy)](ClO_4)_2$ (**2**), $[Cr(OH_2)(Cat)(trpy)]ClO_4$ (**3**), $[Cr(OH_2)(Cl_4Cat)(trpy)]ClO_4$ (**4**), $[Cr(OH_2)(3,5\text{-}Bu_2SQ)(Me_3\text{-}tacn)](ClO_4)_2$ (**5**), $[Cr(OH_2)(Cat)(Me_3\text{-}tacn)]ClO_4$ (**6**), and $[Cr(OH_2)(Cl_4Cat)(Me_3\text{-}tacn)]ClO_4$ (**7**) (Bu_2SQ = di-*tert*-butyl-*o*-benzosemiquinonate anion, Bu_2Cat = di-*tert*-butylcatecholate dianion, Cat = catecholate dianion, Cl_4Cat = tetrachlorocatecholate dianion, trpy = 2,2′:6′,2″-terpyridine, and Me_3-tacn = 1,4,7-trimethyl-1,4,7-triazacyclononane), were prepared. On the basis of the crystal structures, redox behavior, and elemental analyses of these complexes, dioxolene in **1c**, **3**, **4**, **6**, and **7** coordinated to Cr(III) as the catechol form, and the ligand in **1s**, **2**, and **5** was linked to Cr(III) with the semiquinone form. All the aqua–Cr(III) complexes reversibly changed to the hydroxo–Cr(III) ones upon dissociation of the aqua proton, and the pK_a value of the aqua–Cr(III) complexes increased in the order **6** > **3** ≈ **1c** > **7** > **5** ≈ **4** > **1s**. Hydroxo–Cr(III)–catechol complexes derived from **1c**, **3**, **4**, **6**, and **7** did not show any signs of dissociation of their hydroxy proton. On the other hand, hydroxo–Cr(III)–semiquinone complexes were reduced to hydroxo–Cr(III)–catechol in H_2O/THF at pH 11 under illumination of visible light.

Introduction

Regulation of reactivity of oxo groups ligated on metals has been a fascinating subject in biological and catalytic oxidation reactions. High-valent $M_2(\mu\text{-}O)_2$ complexes (M = Cu,[1−16] Fe,[17−21] Co,[22,23] and Ni[22,24]) have been obtained by the O−O bond scission of O_2^{2-} on dinuclear metal complexes. The structural conversion between $Cu_2(\mu\text{-}O)_2$ and $Cu_2(\mu\text{-}\eta^2\text{:}\eta^2\text{-}O_2)$ cores is also confirmed at low temperatures.[3] These studies greatly contribute to the elucidation of the chemical properties and reactivity of the $M_2(\mu\text{-}O)_2$ cores. On the other hand, a rational preparative route to metal complexes with terminal oxo ligands through O−O bond cleavage of O_2 has not been presented so far despite the

* To whom correspondence should be addressed. E-mail: ktanaka@ims.ac.jp. Phone: +81-564-55-7241. Fax: +81-564-55-5245.

(1) Mahapatra, S.; Halfen, J. A.; Wilkinson, E. C.; Pan, G.; Cramer, C. J.; Que, L., Jr.; Tolman, W. B. *J. Am. Chem. Soc.* **1995**, *117*, 8865−8866.
(2) Mahapatra, S.; Halfen, J. A.; Wilkinson, E. C.; Pan, G.; Wang, X.; Young, V. G., Jr.; Cramer, C. J.; Que, L., Jr.; Tolman, W. B. *J. Am. Chem. Soc.* **1996**, *118*, 11555−11574.
(3) Halfen, J. A.; Mahapatra, S.; Wilkinson, E. C.; Kaderli, S.; Young, V. G., Jr.; Que, L., Jr.; Zuberbühler, A. D.; Tolman, W. B. *Science* **1996**, *271*, 1397−1400.
(4) Mahapatra, S.; Halfen, J. A.; Tolman, W. B. *J. Am. Chem. Soc.* **1996**, *118*, 11575−11586.
(5) Mahapatra, S.; Kaderli, S.; Llobet, A.; Neuhold, Y.-M.; Palanché, T.; Halfen, J. A.; Young, V. G., Jr.; Kaden, T. A.; Que, L., Jr.; Zuberbühler, A. D.; Tolman, W. B. *Inorg. Chem.* **1997**, *36*, 6343−6356.
(6) Mahapatra, S.; Young, V. G., Jr.; Kaderli, S.; Zuberbühler, A. D.; Tolman, W. B. *Angew. Chem., Int. Ed. Engl.* **1997**, *36*, 130−133.
(7) Tolman, W. B. *Acc. Chem. Res.* **1997**, *30*, 227−237.
(8) Cole, A. P.; Root, D. E.; Mukherjee, P.; Solomon, E. I.; Stack, T. D. P. *Science* **1996**, *273*, 1848−1850.
(9) Mahadevan, V.; Hou, Z.; Cole, A. P.; Root, D. E.; Lal, T. K.; Solomon, E. I.; Stack, T. D. P. *J. Am. Chem. Soc.* **1997**, *119*, 11996−11997.
(10) DuBois, J. L.; Mukherjee, P.; Collier, A. M.; Mayer, J. M.; Solomon, E. I.; Hedman, B.; Stack, T. D. P.; Hodgson, K. O. *J. Am. Chem. Soc.* **1997**, *119*, 8578−8579.
(11) Allen, W. E.; Sorrell, T. N. *Inorg. Chem.* **1997**, *36*, 1732−1734.
(12) Itoh, S.; Nakao, H.; Berreau, L. M.; Kondo, T.; Komatsu, M.; Fukuzumi, S. *J. Am. Chem. Soc.* **1998**, *120*, 2890−2899.
(13) Enomoto, M.; Aida, T. *J. Am. Chem. Soc.* **1999**, *121*, 874−875.
(14) Blain, I.; Bruno, P.; Giorgi, M.; Lojou, E.; Lexa, D.; Réglier, M. *Eur. J. Inorg. Chem.* **1998**, 1297−1304.
(15) Hayashi, H.; Fujinami, S.; Nagatomo, S.; Ogo, S.; Suzuki, M.; Uehara, A.; Watanabe, Y.; Kitagawa, T. *J. Am. Chem. Soc.* **2000**, *122*, 2124−2125.
(16) Hayashi, H.; Uozumi, K.; Fujinami, S.; Nagatomo, S.; Shiren, K.; Furutachi, H.; Suzuki, M.; Uehara, A.; Kitagawa, T. *Chem. Lett.* **2002**, 416−417.
(17) Que, L., Jr. *J. Chem. Soc., Dalton Trans.* **1997**, 3933−3940.
(18) Dong, Y.; Fujii, H.; Hendrich, M. P.; Leising, R. A.; Pan, G.; Randall, C. R.; Wilkinson, E. C.; Zang, Y.; Que, L., Jr.; Fox, B. G.; Kauffmann, K.; Münck, E. *J. Am. Chem. Soc.* **1995**, *117*, 2778−2792.

10.1021/ic020308m CCC: $22.00
Published on Web 10/11/2002

importance of those complexes in many enzymatic oxygenase reactions.[25,26] Accordingly, aqua−Ru complexes have widely been used as precursors to oxo−Ru ones because oxidation of those complexes is accompanied with loss of protons to afford higher oxidation states of hydro− and oxo−Ru ones (eq 1).[27] The accessibility to the higher oxidation states of

$$[Ru^{II}(OH_2)(bpy)(trpy)]^{2+} \xrightarrow{-e^-,\ -H^+} [Ru^{III}(OH)(bpy)(trpy)]^{2+} \xrightarrow{-e^-,\ -H^+} [Ru^{IV}(O)(bpy)(trpy)]^{2+} \quad (1)$$

the complexes is attributable to electron donation from bound hydroxo or oxo ligands. In addition, the higher oxidation state oxo−Ru complexes thus formed have proven to work as stoichiometric and catalytic oxidants.[28−30] Recently, we have shown that replacement of bpy of $[Ru(OH_2)(bpy)(trpy)]^{2+}$ with quinone as an electron acceptor greatly enhances the acidity of the aqua ligand.[31−34] Moreover, monomeric and dimeric oxo−Ru complexes derived from aqua−Ru ones showed high catalytic activity for some dehydrogenation reactions[32] and four-electron oxidation of water.[33,34] Along the line, we also examined the reactivity and physical properties of aqua−, hydroxo−, and oxo−chromium(III)−dioxolene complexes. Here, we report the synthesis of a series of aqua−Cr−dioxolene complexes, $[Cr(OH_2)(3,5\text{-}Bu_2SQ)(trpy)](ClO_4)_2$ (**1s**), $[Cr(OH_2)(3,5\text{-}Bu_2Cat)(trpy)]ClO_4$ (**1c**), $[Cr(OH_2)(3,6\text{-}Bu_2SQ)(trpy)](ClO_4)_2$ (**2**), $[Cr(OH_2)(Cat)(trpy)]ClO_4$ (**3**), $[Cr(OH_2)(Cl_4Cat)(trpy)]ClO_4$ (**4**), $[Cr(OH_2)(3,5\text{-}Bu_2SQ)(Me_3\text{-}tacn)](ClO_4)_2$ (**5**), $[Cr(OH_2)(Cat)(Me_3\text{-}tacn)]ClO_4$ (**6**), and $[Cr(OH_2)(Cl_4Cat)(Me_3\text{-}tacn)]ClO_4$ (**7**)[35] aimed at smooth conversion to oxo−Cr(III) ones.

Experimental Section

WARNING! Perchlorate salts are potentially explosives and should only be handled in small quantities.

Materials. All reagents and solvents were commercially available and used without further purification.

$[Cr(OH_2)(3,5\text{-}Bu_2SQ)(trpy)](ClO_4)_2\cdot 3(CH_3OH)$ (1s). A mixture of $[CrCl_3(trpy)]$[36] (392 mg, 1.0 mmol) and $AgClO_4$ (622 mg, 3.0 mmol) was refluxed in methanol (30 cm^3) for 6 h, and precipitated AgCl was removed by filtration. To the brown filtrate (**A**) was added 3,5-di-*tert*-butylcatechol (222 mg, 1.0 mmol) and sodium hydroxide (80 mg, 2.0 mmol), and then the solution was stirred for 6 h under N_2. Acidification of the solution by an addition of 0.2 cm^3 of $HClO_4$ (70%) and the subsequent treatment with $AgClO_4$ (207 mg, 1.0 mmol) brought about a change in color of the solution from dark brown to green. After filtration of the solution to remove Ag, water (10 cm^3) was added to the filtrate. Slow evaporation of the solvent yielded a green needle crystalline precipitate, which was filtered off, washed with water, and air-dried. Yield: 539 mg (66%). Anal. Calcd for $C_{29}H_{33}N_3O_{11}Cl_2Cr\cdot 3(CH_3OH)$: C, 46.95; H, 5.54; N, 5.13. Found: C, 47.26; H, 5.18; N, 4.98. UV−vis (λ_{max}/nm (ϵ/mol^{-1} dm^3 cm^{-1}) in 1 mmol dm^{-3} $HClO_4$ at 25 °C): 281 (17200), 328 (11500, sh), 337 (11600), 403 (5360), 432 (5070), 461 (6320), 520 (450, sh), 632 (450), 685 (950), 875 (230, br), 990 (150).

$[Cr(OH_2)(3,5\text{-}Bu_2Cat)(trpy)]ClO_4\cdot 2(CH_3OH)$ (1c). An aqueous solution (10 cm^3) of l(+)-ascorbic acid (88 mg, 0.5 mmol) was added to a methanolic solution (30 cm^3) of **1s** (409 mg, 0.5 mmol) with stirring at 0 °C under N_2. The mixture was stirred for 5 min, and then 3 drops of $HClO_4$ (70%) were added. Concentration of the solution under N_2 gave **1c** as a brown precipitate. Yield: 175 mg (51%). Anal. Calcd for $C_{29}H_{33}N_3O_7ClCr\cdot 2(CH_3OH)$: C, 54.19; H, 6.01; N, 6.11. Found: C, 53.98; H, 5.98; N, 6.21. UV−vis (λ_{max}/nm (ϵ/mol^{-1} dm^3 cm^{-1}) in 1 mmol dm^{-3} $HClO_4$ at 25 °C): 282 (16200), 325 (11100).

Single crystals suitable for X-ray crystallography were obtained as follows: To a methanolic solution (30 cm^3) of **1c** (50 mg, 0.08 mmol) was added $H_2$3,5-Bu_2Cat (22 mg, 0.10 mmol), 3 drops of $HClO_4$ (70%), and 10 cm^3 of water. Slow evaporation of the solvent under N_2 gave the 1:1 adduct of **1c** with 3,5-di-*tert*-butylcatechol ($[Cr(OH_2)(3,5\text{-}Bu_2Cat)(trpy)]ClO_4\cdot H_2$3,5-$Bu_2Cat\cdot CH_3OH$ (**1c′**)) as large brown crystals. Yield: 58 mg (83%). Anal. Calcd for $C_{29}H_{33}N_3O_7ClCr\cdot C_{14}H_{22}O_2\cdot CH_3OH$: C, 60.23; H, 6.78; N, 4.79. Found: C, 59.99; H, 6.88; N, 4.71.

$[Cr(OH_2)(3,6\text{-}Bu_2SQ)(trpy)](ClO_4)_2\cdot CH_3OH\cdot H_2O$ (2). This complex was obtained as green crystals in a manner similar to that of **1s** except that 3,6-di-*tert*-butylcatechol[37] was used in place of 3,5-di-*tert*-butylcatechol. Additions of water (10 cm^3), 3 drops of $HClO_4$ (70%) and $NaClO_4$ (10 mg, 0.08 mmol) to a methanolic solution (10 cm^3) of **2** (100 mg, 0.13 mmol) gave green crystals suitable for X-ray crystallography. Yield: 426 mg (55%). Anal. Calcd for $C_{29}H_{33}N_3O_{11}Cl_2Cr\cdot CH_3OH\cdot H_2O$: C, 46.64; H, 5.09; N, 5.44. Found: C, 46.75; H, 5.02; N, 5.38. This complex was stable in the solid state but slowly decomposed in solutions.

$[Cr(OH_2)(Cat)(trpy)]ClO_4\cdot H_2O$ (3). To a methanolic solution of **A** (same scale as **1s**) was added catechol (110 mg, 1.0 mmol) and sodium hydroxide (80 mg, 2.0 mmol) under N_2. The mixture was stirred for 6 h, and then 0.2 cm^3 of $HClO_4$ (70%) and 10 cm^3 of water were added to the solution. Evaporation of the solvent

(19) Kim, C.; Dong, Y.; Que, L., Jr. *J. Am. Chem. Soc.* **1997**, *119*, 3635−3636.
(20) Dong, Y.; Que, L., Jr.; Kauffmann, K.; Münck, E. *J. Am. Chem. Soc.* **1995**, *117*, 11377−11378.
(21) Dong, Y.; Zang, Y.; Shu, L.; Wilkinson, E. C.; Que, L., Jr.; Kauffmann, K.; Münck, E. *J. Am. Chem. Soc.* **1997**, *119*, 12683−12684.
(22) Hikichi, S.; Yoshizawa, M.; Sasakura, Y.; Akita, M.; Moro-oka, Y. *J. Am. Chem. Soc.* **1998**, *120*, 10567−10568.
(23) Hikichi, S.; Komatsuzaki, H.; Akita, M.; Moro-oka, Y. *J. Am. Chem. Soc.* **1998**, *120*, 4699−4710.
(24) Shiren, K.; Ogo, S.; Fujinami, S.; Hayashi, H.; Suzuki, M.; Uehara, A.; Watanabe, Y.; Moro-oka, Y. *J. Am. Chem. Soc.* **2000**, *122*, 254−262.
(25) Special thematic issue for metal−dioxygen complexes: *Chem. Rev.* **1994**, *94*, 567−856 and references therein.
(26) Special thematic issue for oxygen metabolism in bioinorganic enzymology: *Chem. Rev.* **1996**, *96*, 2541−2950 and references therein.
(27) Takeuchi, K. J.; Thompson, M. S.; Pipes, D. W.; Meyer, T. J. *Inorg. Chem.* **1984**, *23*, 1845−1851.
(28) Seok, W. K.; Dobson, J. C.; Meyer, T. J. *Inorg. Chem.* **1988**, *27*, 3−5.
(29) Che, C.-M.; Tang, W.-T.; Lee, W.-O.; Wong, K.-Y.; Lau, T.-C. *J. Chem. Soc., Dalton Trans.* **1992**, 1551−1556.
(30) Lebeau, E. L.; Meyer, T. J. *Inorg. Chem.* **1999**, *38*, 2174−2181.
(31) Tsuge, K.; Kurihara, M.; Tanaka, K. *Bull. Chem. Soc. Jpn.* **2000**, *73*, 607−614.
(32) Wada, T.; Tsuge, K.; Tanaka, K. *Chem. Lett.* **2000**, 910−911.
(33) Wada, T.; Tsuge, K.; Tanaka, K. *Angew. Chem., Int. Ed.* **2000**, *39*, 1479−1482.
(34) Wada, T.; Tsuge, K.; Tanaka, K. *Inorg. Chem.* **2001**, *40*, 329−337.

(35) Abbreviations of ligands used: Bu_2SQ = di-*tert*-butyl-*o*-benzosemiquinonate anion, Bu_2Cat = di-*tert*-butylcatecholate dianion, Cat = catecholate dianion, Cl_4Cat = tetrachlorocatecholate dianion, trpy = 2, 2′: 6′, 2″-terpyridine, Me_3-tacn = 1,4,7-trimethyl-1,4,7-triazacyclononane, bpy = 2, 2′-bipyridine, acac = acetylacetonate anion, tren = tris(2-aminoethyl)amine, and CTH = (±)5,7,7,12,14,14-hexamethyl-1,4,8,11-tetraazacyclotetradecane.

(36) Broomhead, J. A.; Evans, J.; Grumley, W. D.; Sterns, M. *J. Chem. Soc., Dalton Trans.* **1976**, 173−176.
(37) Belostotskaya, I. S.; Komissarova, N. L.; Dzhuaryan, E. V.; Ershov, V. V. *Isv. Akad. Nauk SSSR* **1972**, 1594−1596.

under N_2 stream afforded brown crystals suitable for X-ray diffraction. Yield: 372 mg (70%). Anal. Calcd for $C_{21}H_{17}N_3O_7ClCr\cdot H_2O$: C, 47.69; H, 3.62; N, 7.95. Found: C, 47.75; H, 3.74; N, 7.82. UV−vis (λ_{max}/nm (ϵ/mol^{-1} dm^3 cm^{-1}) in 1 mmol dm^{-3} $HClO_4$ at 25 °C): 288 (19500), 334 (14000), 350 (12000, sh), 650 (100).

[Cr(OH$_2$)(Cl$_4$Cat)(trpy)]ClO$_4$·H$_2$O (4). Tetrachlorocatechol (248 mg, 1.0 mmol) and sodium hydroxide (80 mg, 2.0 mmol) were added to a methanolic solution of **A** (same scale as **1s**). The mixture was stirred for 6 h, and then 0.2 cm^3 of $HClO_4$ (70%) was added to the suspension. After insoluble precipitate was removed by filtration, the brown filtrate was allowed to stand for several days to give brown crystals suitable for X-ray crystallography. Yield: 391 mg (59%). Anal. Calcd for $C_{21}H_{13}N_3O_{10}Cl_5Cr\cdot H_2O$: C, 37.84; H, 2.27; N, 6.30. Found: C, 38.10; H, 2.27; N, 6.30. UV−vis (λ_{max}/nm (ϵ/mol^{-1} dm^3 cm^{-1}) in 1 mmol dm^{-3} $HClO_4$ at 25 °C): 283 (13300), 327 (11100), 343 (10500, sh).

[Cr(OH$_2$)(3,5-Bu$_2$SQ)(Me$_3$-tacn)](ClO$_4$)$_2$·H$_2$O (5). This complex was obtained as a green polycrystalline solid in a manner similar to that of **1s** except that [$CrCl_3$(Me$_3$-tacn)][38] was used instead of [$CrCl_3$(trpy)]. Yield: 315 mg (46%). Anal. Calcd for $C_{23}H_{43}N_3O_{11}Cl_2Cr\cdot H_2O$: C, 40.71; H, 6.68; N, 6.19. Found: C, 40.50; H, 6.57; N, 6.09. UV−vis (λ_{max}/nm (ϵ/mol^{-1} dm^3 cm^{-1}) in 1 mmol dm^{-3} $HClO_4$ at 25 °C): 274 (7300), 338 (3000), 386 (4000), 450 (4300), 520 (330, sh), 602 (380), 685 (1200), 816 (180, br), 878 (190, br), 1000 (130, sh).

[Cr(OH$_2$)(Cat)(Me$_3$-tacn)]ClO$_4$·H$_2$O (6). The compound was obtained as green prism crystals by a method similar to that of **3** except that [$CrCl_3$(Me$_3$-tacn)] was used instead of [$CrCl_3$(trpy)]. Yield: 294 mg (63%). Anal. Calcd for $C_{15}H_{27}N_3O_7ClCr\cdot H_2O$: C, 38.59; H, 6.26; N, 9.00. Found: C, 38.39; H, 6.28; N, 8.99. UV−vis (λ_{max}/nm (ϵ/mol^{-1} dm^3 cm^{-1}) in 1 mmol dm^{-3} $HClO_4$ at 25 °C): 276 (4900), 300 (2700, sh), 335 (1600), 602 (55).

[Cr(OH$_2$)(Cl$_4$Cat)(Me$_3$-tacn)]ClO$_4$ (7). This complex was prepared by the same method as that of **4** except that [$CrCl_3$(Me$_3$-tacn)] was used instead of [$CrCl_3$(trpy)]. Green prism[39] and/or hexagon plate crystals[40] were obtained. Yield: 284 mg. The mixture was manually separated. Anal. Calcd for green prism crystals ($C_{15}H_{23}N_3O_7Cl_5Cr\cdot H_2O$): C, 29.80; H, 4.17; N, 6.95. Found: C, 29.75; H, 4.20; N, 6.90. Anal. Calcd for green hexagon plate crystals ($C_{15}H_{23}N_3O_7Cl_5Cr\cdot CH_3OH$): C, 31.06; H, 4.40; N, 6.79. Found: C, 30.94; H, 4.36; N, 6.80. UV−vis (λ_{max}/nm (ϵ/mol^{-1} dm^3 cm^{-1}) in 1 mmol dm^{-3} $HClO_4$ at 25 °C): 285 (5500), 327 (4200).

The crude product was allowed to stand in water/methanol (9:1 v/v), and one green needle crystal (10 × 0.2 × 0.2 mm^3) as [Cr(OH$_2$)(Cl$_4$Cat)(Me$_3$-tacn)]ClO$_4$·2(H$_2$O) (**7′**) suitable for X-ray crystallography was obtained after 2 weeks.

Physical Measurements. Electronic spectra were measured on a Shimadzu UV−vis−NIR scanning spectrophotometer UV-3100PC. Cyclic voltammetric experiments were carried out in a one-compartment cell consisting of a glassy carbon working electrode, a platinum wire auxiliary electrode, and a Ag/AgCl or Ag/Ag$^+$ reference electrode. An ASL model 660 electrochemical analyzer was used to collect the electrochemical data. Magnetic susceptibilities were measured by a SQUID susceptometer, QUANTUM DESIGN MPMS model. Diamagnetic correction was made using Pascal's constants.[41]

X-ray Crystallography. General Procedures. Data were collected on a Rigaku/MSC Mercury CCD diffractometer using graphite monochromated Mo Kα radiation (λ = 0.71070 Å). To determine the cell constants and the orientation matrix, four oscillation photographs were taken with an oscillation angle of 0.5°. Intensity data were collected at a temperature of −100 ± 1 °C to a maximum 2θ value of 55.0°. A total of 720 oscillation images were collected. The first sweep of data was done using ω scans from −70.0 to 110.0° in 0.5° step, at χ = 45.0° and ϕ = 0.0°. The second sweep of data was done using ω scans from −70.0 to 110.0° in 0.5° step, at χ = 45.0° and ϕ = 90.0°. The detector swing angle was 20.0°. The crystal-to-detector distance was 45.0 mm.

The structure was solved by heavy-atom Patterson methods[42] and expanded using Fourier techniques.[43] The non-hydrogen atoms were refined anisotropycally. Hydrogen atoms were included but not refined. All calculations were performed using the teXsan[44] crystallographic software package of Molecular Structure Corporation.

Crystallographic data are summarized in Table 1. Tables of final atomic coordinates, thermal parameters, and full bond distances and angles are given in Supporting Information.

Results and Discussion

Crystal Structures of 1c′−4, 6, and 7′. Figures 1 and 2 show the crystal structures of the complex cations of **1c′** and **6**, respectively (those of **3**, **4**, and **7′** are given in Figures S3, S4, and S6 in Supporting Information). The selected bond distances of **1c′**, **3**, **4**, **6**, and **7′** are given in Table 2. These complexes consist of the chromium cation unit, one counter perchlorate, and solvated molecule(s). The chromium atoms adopt a distorted octahedral structure with three nitrogen atoms of trpy or Me$_3$-tacn, two oxygen of dioxolene, and one water oxygen. The aqua group of the complexes is connected to water, methanol, and/or perchlorate anion with hydrogen bonding. Complexes **3** and **6** exist as dimeric forms in the solid state, because one of the dioxolene oxygens is linked to the aqua ligand of the neighboring complex with hydrogen bonding (Figure 2). The O···O and Cr···Cr distances in the dimer unit are 2.572(2) and 4.954(0) Å for **3** and 2.686(2) and 5.370(1) Å for **6**, respectively. For the complex **1c′**, an additional 3,5-di-*tert*-butylcatechol molecule is bonded to one of the coordinated dioxolene oxygen with a hydrogen bond, as shown in Figure 1.

Each chromium−terminal nitrogen bond distance of trpy of **1c′**, **3**, and **4** (2.074−2.080 Å) is slightly longer than the chromium−central one of those complexes (1.994−2.013 Å), probably because of steric distortion of the chromium trpy complexes. On the other hand, three Cr−N bond distances

(38) Wieghardt, K.; Chaudhuri, P.; Nuber, B.; Weiss, J. *Inorg. Chem.* **1982**, *21*, 3086−3090.

(39) Crystal data for **7**·H$_2$O: $C_{15}H_{23}N_3O_7Cl_5Cr\cdot H_2O$, monoclinic, $P2_1/n$, a = 8.471(5) Å, b = 8.491(5) Å, c = 33.23(2) Å, β = 96.546(7)°, V = 2374(2) Å^3, Z = 4, D_c = 1.691 g/cm^3, R = 0.088, R_w = 0.185.

(40) Crystal data for **7**·CH$_3$OH: $C_{15}H_{23}N_3O_7Cl_5Cr\cdot CH_3OH$, monoclinic, $P2_1/a$, a = 16.983(2) Å, b = 8.212(2) Å, c = 19.873(1) Å, β = 114.186(7)°, V = 2528.1(7) Å^3, Z = 4, D_c = 1.625 g/cm^3, R = 0.135, R_w = 0.250.

(41) Mabbs, F. E.; Marchin, D. J. *Magnetisms and Transition Metal Complexes*; Chapman and Hall: London, 1975; p 5.

(42) PATTY: Beurskens, P. T.; Admiraal, G.; Beurskens, G.; Bosman, W. P.; de Gelder, R.; Israel, R.; Smits, J. M. M. *The DIRDIF-94 program system*; Technical Report of the Crystallography Laboratory; University of Nijmegen, The Netherlands, 1994.

(43) DIRDIF94: Beurskens, P. T.; Admiraal, G.; Beurskens, G.; Bosman, W. P.; de Gelder, R.; Israel, R; Smits, J. M. M. *The DIRDIF-94 program system*; Technical Report of the Crystallography Laboratory; University of Nijmegen, The Netherlands, 1994.

(44) teXsan: *Crystal Structure Analysis Package*; Molecular Structure Corporation, 1985 & 1992.

Table 1. Crystallographic Data for **1c′**−**4**, **6**, and **7′**

	1c′	**2**	**3**	**4**	**6**	**7′**
formula	$CrC_{44}H_{59}N_3O_{10}Cl$	$CrC_{30}H_{39}N_3O_{13}Cl_2$	$CrC_{21}H_{19}N_3O_8Cl$	$CrC_{21}H_{15}N_3O_8Cl_5$	$CrC_{15}H_{29}N_3O_8Cl$	$CrC_{15}H_{27}N_3O_9Cl_5$
fw	877.41	772.55	528.85	666.63	466.86	622.65
temp, °C	−100	−100	−100	−100	−100	−100
cryst dimensions, mm^3	0.25 × 0.15 × 0.50	0.15 × 0.15 × 0.50	0.40 × 0.40 × 0.50	0.20 × 0.50 × 0.50	0.30 × 0.30 × 0.40	0.45 × 0.20 × 0.20
cryst syst	monoclinic	orthorhombic	monoclinic	monoclinic	monoclinic	orthorhombic
space group	$P2_1/a$ (No. 14)	$Pna2_1$ (No. 33)	$C2/c$ (No. 15)	$P2_1/a$ (No. 14)	$P2_1/c$ (No. 14)	$P2_12_12_1$ (No. 19)
a, Å	12.106(4)	22.058(2)	24.764(2)	12.473(1)	9.2492(8)	8.4891(5)
b, Å	15.625(5)	13.3259(9)	13.300(1)	12.2879(8)	15.663(1)	15.2677(9)
c, Å	24.315(8)	12.4739(8)	13.915(1)	17.138(1)	14.005(1)	19.067(1)
β, deg	100.984(4)	90	108.408(3)	104.080(4)	95.704(5)	90
V, $Å^3$	4514(2)	3666.7(8)	4348.4(6)	2547.8(4)	2018.9(3)	2471.2(3)
Z	4	4	8	4	4	4
$2\theta_{max}$	55	55	55	55	55	55
$F(000)$	1860	1608	2168	1340	980	1276
D_{calcd}, g/cm^3	1.291	1.399	1.615	1.738	1.536	1.673
abs coeff, cm^{-1}	3.71	5.22	7.05	10.26	7.46	10.53
no. reflns (all, $2\theta < 55°$)	10088	4369	4950	5805	4482	3188
no. variables	532	443	307	343	253	298
GOF	1.70	1.61	1.89	1.73	1.69	1.62
largest peak/hole, e $Å^{-3}$	0.75/−0.61	0.39/−0.35	0.66/−0.72	1.07/−0.63	0.68/−0.52	0.40/−0.31
R1[a] [$I > 2\sigma(I)$]	0.082	0.061	0.057	0.056	0.048	0.031
R^b (all data)	0.083	0.083	0.069	0.069	0.058	0.039
$R_w{}^c$ (all data)	0.166	0.171	0.159	0.156	0.129	0.080

[a] $R1 = \sum[|F_o| - |F_c|]/\sum|F_o|$. [b] $R = \sum[F_o^2 - F_c^2]/\sum F_o^2$. [c] $R_w = [(\sum w(F_o^2 - F_c^2)^2/\sum w(F_o^2)^2)]^{1/2}$.

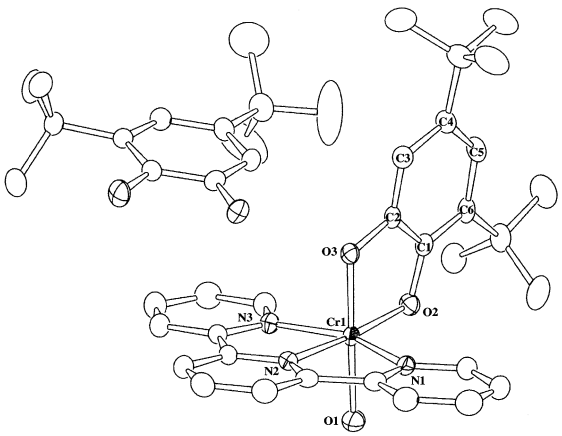

Figure 1. ORTEP views (50% probability) of complex cation and free dioxolene of **1c′**. Hydrogen atoms are omitted for clarity.

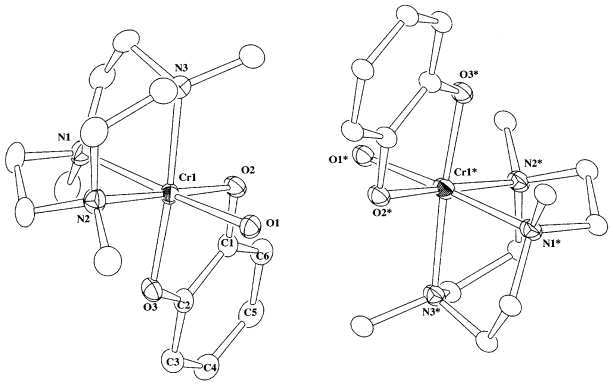

Figure 2. ORTEP view (50% probability) of complex cations of **6**. Hydrogen atoms are omitted for clarity.

of Me_3-tacn complexes **6** and **7′** are almost the same, and the average is 2.104 Å. The chromium−oxygen bond length of dioxolene of **1c′**, **3**, **4**, **6**, and **7′** is in the range 1.916−1.940 Å, and the distance is shorter than that of the Cr(III)−triscatechol complex, $K_3[Cr(Cat)_3]$ ($Cr-O_{av} = 1.986$ Å).[45] The Cr−O(aqua) bond distance of these complexes ranges from 2.015 to 2.036 Å and is close to the $Cr-OH_2$ bond distance of $[Cr(OH_2)(acac)(Me_3\text{-tacn})]^{2+}$ (Cr−O = 2.067-(6) Å).[46] These bond lengths apparently are longer than the Cr−OH bond of $[Cr(OH)(acac)(Me_3\text{-tacn})]^+$ (Cr−O = 1.90-(2) Å).[47] Nearly identical C−C bond lengths in dioxolene ligands (Table 2) are implications of the aromatic nature of the C6 ring. In fact, the C−O bond length of **1c′**, **3**, **4**, **6**, and **7′** in the range 1.333−1.352 Å is close to that of free catechol[48] and $K_3[Cr(Cat)_3]$[45] ($C-O_{av} = 1.371$ and 1.346 Å,

Table 2. Selected Bond Distances (Å) of **1c′**−**4**, **6**, and **7′**

	1c′	**1c′**[a]	**2**	**3**	**4**	**6**	**7′**
Cr1−O1	2.032(2)		1.980(3)	2.015(2)	2.031(2)	2.036(2)	2.032(2)
Cr1−O2	1.898(2)		1.906(4)	1.936(2)	1.921(2)	1.945(2)	1.936(2)
Cr1−O3	1.933(2)		1.923(3)	1.925(2)	1.924(2)	1.935(2)	1.915(2)
Cr1−N1	2.080(2)		2.064(5)	2.071(2)	2.071(2)	2.101(2)	2.086(3)
Cr1−N2	2.013(2)		1.985(4)	1.994(2)	2.005(2)	2.112(2)	2.099(3)
Cr1−N3	2.080(2)		2.065(4)	2.080(2)	2.076(2)	2.118(2)	2.110(3)
O2−C1	1.361(3)	1.379(3)[a]	1.317(5)	1.365(3)	1.331(3)	1.366(3)	1.335(4)
O3−C2	1.377(3)	1.387(3)[a]	1.289(6)	1.359(3)	1.334(3)	1.364(3)	1.331(4)
C1−C2	1.410(4)	1.394(4)[a]	1.452(6)	1.405(3)	1.423(4)	1.412(3)	1.413(5)
C1−C6	1.397(4)	1.393(4)[a]	1.419(6)	1.380(3)	1.387(4)	1.388(3)	1.391(4)
C2−C3	1.381(4)	1.395(4)[a]	1.424(7)	1.389(3)	1.395(4)	1.385(3)	1.392(4)
C3−C4	1.403(4)	1.399(4)[a]	1.380(7)	1.391(4)	1.384(4)	1.395(3)	1.400(4)
C4−C5	1.397(4)	1.397(4)[a]	1.416(8)	1.385(4)	1.407(4)	1.388(3)	1.389(5)
C5−C6	1.407(4)	1.389(4)[a]	1.389(7)	1.393(4)	1.402(4)	1.395(3)	1.402(4)
Cr1···Cr1*				4.954(0)		5.370(1)	
O1···O2*				2.572(2)		2.686(2)	

[a] Bond distances of an additional 3,5-dibutylcatechol molecule.

(45) Raymond, K. N.; Isied, S. S.; Brown, L. D.; Fronczed, F. R.; Nibert, J. H. *J. Am. Chem. Soc*. **1976**, *98*, 1767−1774.
(46) Bossek, U.; Haselhorst, G.; Ross, S.; Wieghardt, K.; Nuber, B. *J. Chem. Soc., Dalton Trans*. **1994**, 2041−2048.
(47) Bossek, U.; Wieghardt, K.; Nuber, B.; Weiss, J. *Angew. Chem., Int. Ed. Engl.* **1990**, *29*, 1055−1057.
(48) Wunderlich, H.; Mootz, D. *Acta Crystallogr*. **1971**, *B27*, 1684−1686.

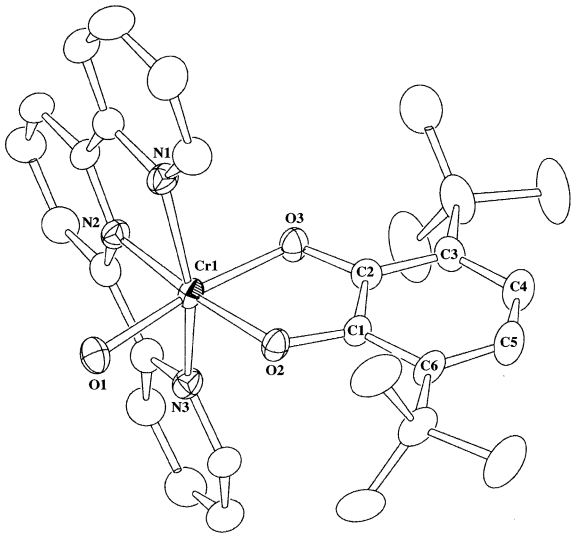

Figure 3. ORTEP view (50% probability) of a complex cation of **2**. Hydrogen atoms are omitted for clarity.

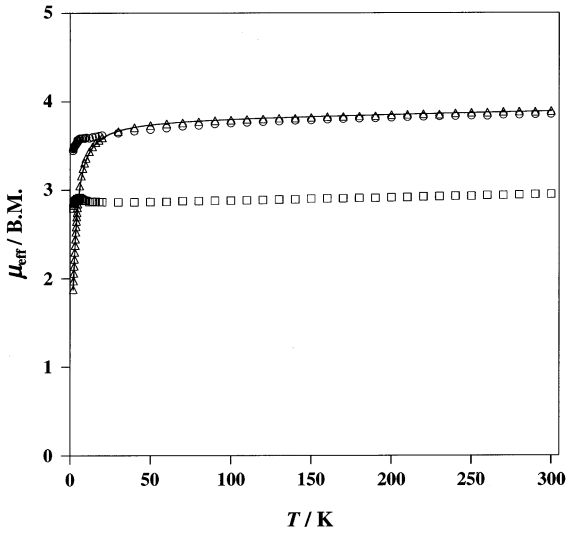

Figure 4. Temperature dependencies of the effective magnetic moments of **1c′** (○), **2** (□), and **3** (△). The solid line represents the best fit of the data for **3** (see text).

respectively). The geometry of the C6 ring of free dioxolene unit of **1c′** ($C-C_{av}$ = 1.395, $C-O_{av}$ = 1.383 Å) is also comparable to the catechol structure.[48] The dioxolene ligand of **1c′**, **3**, **4**, **6**, and **7′**, therefore, is linked to Cr(III) with the catechol form.

The structure of the complex cation of **2** is shown in Figure 3. The selected bond distances of **2** are given in Table 2. The external view of the complex cation of **2** is similar to that of catechol complexes **1c′**, **3**, and **4**, though **2** has two counter perchlorate ions per one cation unit. The average Cr−O(dioxolene) and Cr−N(terminal) bond lengths of **2** are 1.915 and 2.065 Å, respectively, which are comparable to those of **1c′**, **3**, and **4**. On the other hand, the distances of the Cr−O(aqua) and Cr−N(central) bonds of **2**, which are in *trans* positions of oxygen atoms of dioxolene, are 1.980(3) and 1.985(4) Å, respectively, and these bond lengths are slightly shorter than those of **1c′**, **3**, and **4**. The average C−O bond distance (1.303 Å) of **2** is different from that of free catechol ($C-O_{av}$ = 1.371 Å)[48] and *o*-benzoquinone (C−O = 1.220 Å)[49] and comparable to that of Cr(III) semiquinone complexes, [Cr(tren)(3,6-Bu_2SQ)]$(PF_6)_2$,[50] [Cr(3,5-Bu_2SQ)$_3$],[51] and [Cr(Cl_4SQ)$_3$][52] ($C-O_{av}$ = 1.303, 1.285, and 1.28 Å, respectively). Moreover, the dioxolene C6 ring has two short C3−C4 and C5−C6 bonds ($C-C_{av}$ = 1.385 Å) and four long C1−C2, C1−C6, C2−C3, and C4−C5 bonds ($C-C_{av}$ = 1.428 Å) which are similar to those of semiquinone complexes.[50−52] On the basis of these geometrical patterns, the electronic structure of **2** is characterized as an aqua−Cr(III)−semiquinone complex, $[Cr^{III}(OH_2)(3,6\text{-}Bu_2SQ)(trpy)]^{2+}$.

Magnetic Studies. Magnetic susceptibility data for powdered samples of **1**−**7** were collected in the temperature region 2−300 K. Plots of temperature dependence of the effective magnetic moments (μ_{eff}) of **1c′**−**3** are given in Figure 4, and magnetic data for **1**−**7** are summarized in Table 3.

Table 3. Magnetic Data for **1**−**7**

complex	μ_{eff}/μ_B[a]	g	J/cm^{-1}	ref
[Cr(OH_2)(3,5-Bu_2SQ)(trpy)]$^{2+}$ (**1s**)	2.87			*b*
[Cr(OH_2)(3,5-Bu_2Cat)(trpy)]$^{+}$ (**1c′**)	3.85			*b*
[Cr(OH_2)(3,6-Bu_2SQ)(trpy)]$^{2+}$ (**2**)	2.95			*b*
[Cr(OH_2)(Cat)(trpy)]$^{+}$ (**3**)	3.80 (50−300 K) 1.88 (2 K)	1.97	−0.6	*b*
[Cr(OH_2)(Cl_4Cat)(trpy)]$^{+}$ (**4**)	3.82			*b*
[Cr(OH_2)(3,5-Bu_2SQ)(Me_3-tacn)]$^{2+}$ (**5**)	2.96			*b*
[Cr(OH_2)(Cat)(Me_3-tacn)]$^{+}$ (**6**)	3.79 (50−300 K) 1.69 (2 K)	1.97	−0.8	*b*
[Cr(OH_2)(Cl_4Cat)(Me_3-tacn)]$^{+}$ (**7**)	3.86			*b*
[Cr(tren)(3,6-Bu_2SQ)]$^{2+}$	2.85			45
[Cr(tren)(3,6-Bu_2Cat)]$^{+}$	3.85			45

[a] Average value. [b] This work.

The magnetic moments of **1c′**, **4**, and **7** are almost constant in the temperature region 2−300 K. The average effective magnetic moments of **1c′**, **4**, and **7** were 3.85, 3.82, and 3.86 μ_B, respectively, which agree with the spin-only value of 3.87 μ_B for the Cr(III)−catechol formula (S_{Cr} = $^3/_2$). Complex **3** displayed temperature-dependent effective magnetic moments (Figure 4). In the temperature region 50−300 K, the value of μ_{eff} = 3.80 ± 0.1 μ_B was close to the spin-only value of 3.87 μ_B for S = $^3/_2$. As the temperature was lowered, the magnetic moment gradually decreased and became 1.88 μ_B at 2 K, indicating the presence of a weak antiferromagnetic interaction between two Cr(III)−catechol moieties bridged by two hydrogen bonds in the dimer unit as described previously. The magnetic exchange coupling constant (J) was calculated on the basis of the isotropic spin Hamiltonian $\mathbf{H} = -2J\mathbf{S}_1\cdot\mathbf{S}_2$. The theoretical equation of molar magnetic susceptibility (χ_M) for a monomeric unit is given in eq 2

$$\chi_M = [Ng^2\beta^2/kT][(14 + 5x^6 + x^{10})/(7 + 5x^6 + 3x^{10} + x^{12})] + \text{TIP} \quad (2)$$

(49) Macdonald, A. L.; Trotter, J. *J. Chem. Soc., Perkin Trans. 2* **1973**, 476−480.
(50) Wheeler, D. E.; McCusker, J. K. *Inorg. Chem.* **1998**, *37*, 2296−2307.
(51) Sofen, S. R.; Ware, D. C.; Cooper, S. R.; Raymond, K. N. *Inorg. Chem.* **1979**, *18*, 234−239.
(52) Pierpont, C. G.; Downs, H. H. *J. Am. Chem. Soc.* **1976**, *98*, 4834−4838.

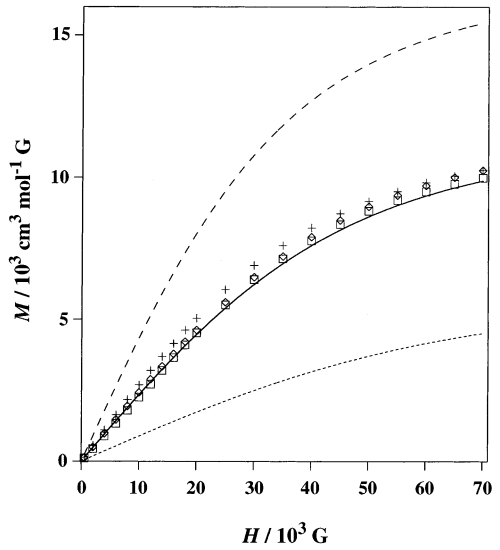

Figure 5. Magnetization M versus magnetic field H plots for **1s** (◇), **2** (□), and **5** (+) at 4.2 K: calculated curve for $S = {}^1/_2$ (·····), calculated curve for $S = 1$ (—), and calculated curve for $S = {}^3/_2$ with $g = 2.0$ (- - -).

where $x = \exp(-J/kT)$, the TIP is a temperature independent paramagnetism which was fixed at 3×10^{-4} cgs emu mol^{-1}, and the other symbols have their usual meanings. The magnetic parameters of **3** are $g = 1.97$ and $J = -0.6$ cm^{-1}. The similar coupling was observed for hydrogen bond bridged dimer **6**. The fitting led to values of $g = 1.97$ and $J = -0.8$ cm^{-1}.

The magnetic moments of **1s**, **2**, and **5** are almost constant. The values of $\mu_{eff} = 2.87$, 2.95, and 2.96 μ_B for **1s**, **2**, and **5**, respectively, agree with the spin-only value of 2.83 μ_B for the $S_T = 1$ state which is confirmed by molar magnetization of **1s**, **2**, and **5** versus magnetic field plots at 4.2 K (Figure 5). These results indicate the strong antiferromagnetic interaction between Cr(III) ($S_{Cr} = {}^3/_2$) and semiquinone ($S_{SQ} = {}^1/_2$). Such a strong antiferromagnetic interaction has been reported for Cr(III)−semiquinone complexes.[50,51,53,54]

Electronic Absorption Spectra. The electronic spectra of $[Cr(OH_2)(3,5\text{-}Bu_2SQ)(trpy)]^{2+}$ (**1s**) show five absorption bands at 401, 431, 463, 630, and 685 nm in the visible region in DME/THF (9:1 v/v) (Figure 6). A similar pattern has been reported in the electronic spectra of Cr(III)−semiquinone complexes such as $[Cr(tren)(3,6\text{-}Bu_2SQ)]^{2+}$ [50] and $[Cr(CTH)(3,6\text{-}Bu_2SQ)]^{2+}$.[53] An addition of small amounts of BuOK in 2-methoxyethanol to the solution resulted in a decrease of the absorbance of these bands and emergence of two new bands at 490 and 735 nm with the appearance of three isosbestic points at 475, 668, and 694 nm. The absorbance of the latter two bands increased with an increase of the amounts of BuOK and reached their maximum intensities in the presence of the equimolar amount of BuOK (Figure 6). The electronic absorption spectrum of the 1:1 mixture of **1s** and BuOK fully changed to that of the original **1s** by an addition of 1 equiv of CF_3SO_3H to the DME/THF solution.

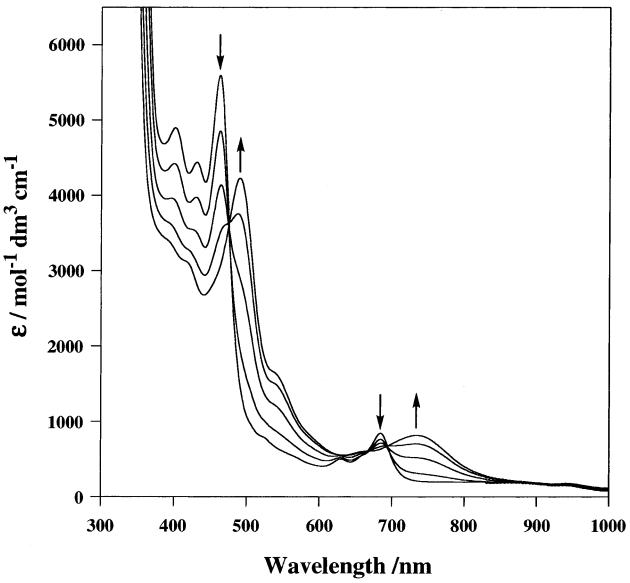

Figure 6. Electronic absorption spectra of $[Cr(OH_2)(3,5\text{-}Bu_2SQ)(trpy)](ClO_4)_2$ in DME/THF (9:1 v/v) containing various amounts of BuOK: $[BuOK]/[Cr(OH_2)(3,5\text{-}Bu_2SQ)(trpy)]^{2+} = 0 - 1.0$ equiv.

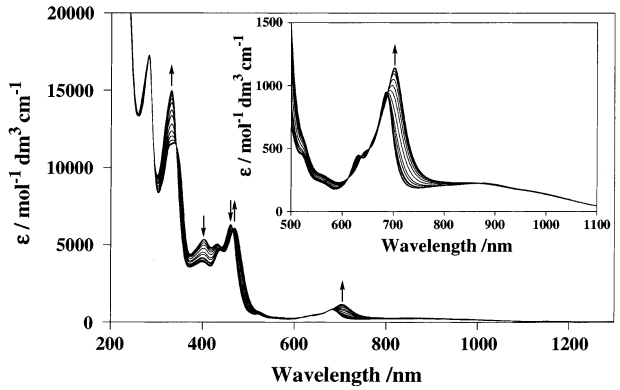

Figure 7. Electronic spectra of $[Cr(OH_2)(3,5\text{-}Bu_2SQ)(trpy)](ClO_4)_2$ depending on pH.

A similar spectral change was observed in aqueous solution. The visible spectra of **1s** at pH 3 in H_2O/THF (9:1 v/v) exhibited several absorption bands at 403, 432, 461, and 685 nm, which decreased with increasing pH, and new bands emerged at 470 and 703 nm (Figure 7). The absorbance of the 470 and 703 nm bands grew up to pH 6 and then became constant in the pH region higher than 7.5. On the basis of the plots of the absorption coefficients at 403, 461, 470, and 703 nm against pH (Figure 8), the pK_a of $[Cr(OH_2)(3,5\text{-}Bu_2SQ)(trpy)]^{2+}$ was determined as 4.5. The pK_a values of the series of the aqua−Cr(III)−semiquinone and −catechol complexes were similarly determined, and the results were summarized in Table 4.

The pK_a values of $[Cr(OH_2)(dioxolene)(trpy)]^{2+}$ are in the range 4.5−6.8, and those of $[Cr(OH_2)(dioxolene)(Me_3\text{-}tacn)]^{2+}$ range from 5.0 to 7.6. Thus, the pK_a of aqua−Cr−Me_3-tacn complexes is larger than the corresponding aqua−Cr−trpy ones by 0.5−1.2. One-electron reduction of **1s** gives rise to an increase in the pK_a value of the aqua ligand by 2.3. An agreement of pK_a of 5.0 between $[Cr(OH_2)(3,5\text{-}Bu_2SQ)(Me_3\text{-}tacn)]^{2+}$ and $[Cr(OH_2)(Cl_4Cat)(trpy)]^{+}$ apparently results from of the compensation of the electron donor ability

(53) Benelli, C.; Dei, A.; Gatteschi, D.; Güdel, H. U.; Pardi, L. *Inorg. Chem.* **1989**, *28*, 3089−3091.
(54) Chang, H.-C.; Miyasaka, H.; Kitagawa, S. *Inorg. Chem.* **2001**, *40*, 146−156.

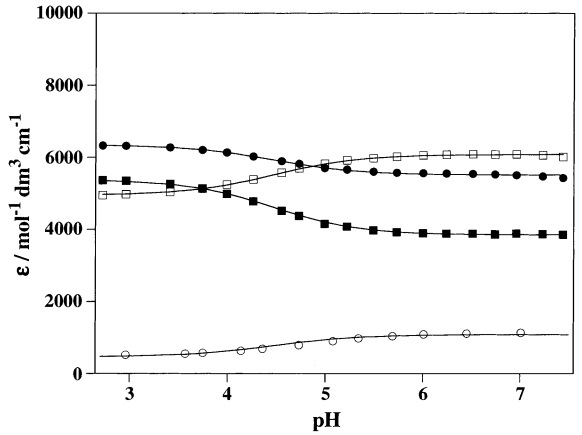

Figure 8. Absorption coefficients at 403 (■), 461 (●), 470 (□), and 703 (○) nm of $[Cr(OH_2)(3,5\text{-}Bu_2SQ)(trpy)](ClO_4)_2$ at various pH values.

Table 4. pK_a Values of the Aqua Complexes $[Cr(OH_2)(dioxolene)(L)]^{n+}$

	dioxolene			
L	3,5-Bu_2SQ	3,5-Bu_2Cat	Cat	Cl_4Cat
trpy	4.5	6.8	6.8	5.0
Me_3-tacn	5.0		7.6	6.2

between Me_3-tacn and trpy and between 3,5-Bu_2SQ and Cl_4-Cat.

The 470 and 703 nm bands of $[Cr(OH)(3,5\text{-}Bu_2SQ)(trpy)]^+$ in H_2O/THF (9:1 v/v) are stable at pH 7, while these bands gradually weakened and finally disappeared to give a featureless electronic absorption spectrum in the visible region at pH 11 for 2 h (Figure 9).

Acidification of the solution does not reproduce the electronic spectrum of **1s**, and the absorption spectrum resembles that of **1c**.[55] Treatment of the resultant solution with 1 equiv of $AgClO_4$ at pH 4 recovered the electronic spectrum of **1s**. On the basis of the facts that the catechol complexes, **1c**, **3**, **4**, **6**, and **7**, did not show any absorption bands in the visible region because of their small absorption coefficients of the d−d transition bands ($\epsilon = 50-120$ mol^{-1} dm^3 cm^{-1}) and oxidation of these catechol complexes with Ag^+ afforded the corresponding semiquinone ones quantitatively, **1s** is reduced to **1c** in H_2O/THF (9:1 v/v) at pH 11. Similarly, $[Cr(OH)(3,5\text{-}Bu_2Cat)(Me_3\text{-}tacn)]^+$ was formed in H_2O/THF solution of the semiquinone complex **5** at pH 11 for 15 h. The reduction in H_2O/THF (9:1 v/v) at pH 11 was greatly enhanced under visible light illumination from a 150 W Xe lamp,[56] and the rate of the reduction proceeded about 20 times faster than that in a cell in a spectrophotometer.

Cyclic Voltammograms. All the aqua−Cr(III)−dioxolene complexes showed one reversible [semiquinone]/[catechol] redox couple in the potential range from −0.8 to +0.8 V (vs SCE) in the cyclic voltammograms in DME/THF (9:1 v/v) and in H_2O/THF (9:1 v/v). As expected from the smooth conversion between the aqua− and hydroxo−Cr(III) complexes, an addition of less than 1 equiv of BuOK to a DME/THF solution of $[Cr(OH_2)(3,5\text{-}Bu_2SQ)(Me_3\text{-}tacn)](ClO_4)_2$ (**5**) caused an appearance of the new [Bu_2SQ]/[Bu_2Cat] redox couple at $E_{1/2} = -0.07$ V (vs SCE) of $[Cr(OH)(3,5\text{-}Bu_2SQ)(Me_3\text{-}tacn)]^+$ at the cost of the peak currents of the [Bu_2SQ]/[Bu_2Cat] redox one at $E_{1/2} = 0.30$ V (vs SCE) of $[Cr(OH_2)(3,5\text{-}Bu_2SQ)(Me_3\text{-}tacn)]^{2+}$. Similarly, all the aqua−Cr(III)−dioxolene complexes were converted to the corresponding hydroxo−Cr(III)−dioxolene ones in the presence of a molar equivalent amount of BuOK, but the [SQ]/[Cat] redox couple of $[Cr(OH)(Cat)(Me_3\text{-}tacn)]$ was not detected because of extremely low solubility of the complex. The redox potentials of the aqua− and hydroxo−Cr(III) complexes thus obtained in DME/THF (9:1 v/v) and in H_2O/THF (9:1 v/v) are summarized in Table 5. It is worthy of note that there is no difference in the patterns of the CV between $[Cr(OH_2)(3,5\text{-}Bu_2SQ)(L)]^{2+}$ and $[Cr(OH_2)(3,5\text{-}Bu_2Cat)(L)]^+$ and between $[Cr(OH)(3,5\text{-}Bu_2SQ)(L)]^+$ and $[Cr(OH)(3,5\text{-}Bu_2Cat)(L)]^0$ (L = trpy, Me_3-tacn), but the rest potentials of the semiquinone and catechol complexes lie at potentials more positive and negative, respectively, than the redox potentials of the [Bu_2SQ]/[Bu_2Cat] couple. In fact, the rest potential of the H_2O/THF (9:1 v/v) solution of $[Cr(OH)(3,5\text{-}Bu_2SQ)(Me_3\text{-}tacn)]^+$ at pH 11 gradually shifted from 0.15 to −0.01 V with retaining the [Bu_2SQ]/[Bu_2Cat] redox couple at $E_{1/2} = 0.10$ V under room light, as shown in Figure 10. It became constant at −0.01 V in 12 h at pH 11.

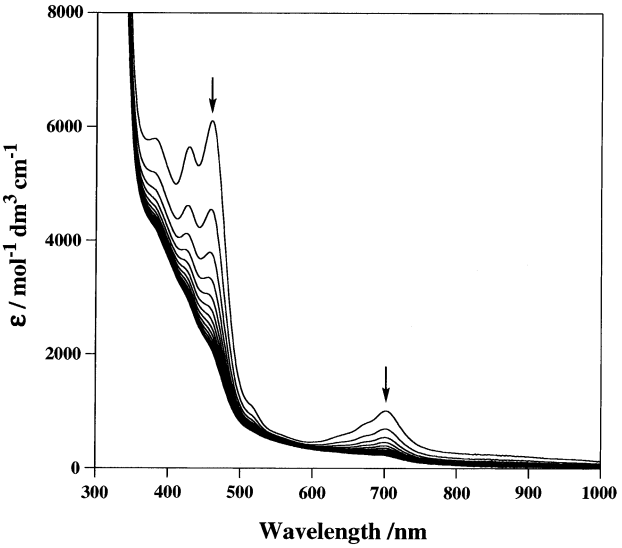

Figure 9. Electronic spectral change of $[Cr(OH)(3,5\text{-}Bu_2SQ)(trpy)]^+$ in H_2O/THF (9:1 v/v) at pH 11.

Table 5. Redox Potential of the [Semiquinone]/[Catechol] Redox Couple of $[Cr(OH_2)(dioxolene)(L)]^{2+}$ and $[Cr(OH)(dioxolene)(L)]^+$ in DME/THF (9:1 v/v) and in H_2O/THF (9:1 v/v)[a]

	3,5-Bu_2SQ		Cat		Cl_4Cat	
L	OH_2	OH	OH_2	OH	OH_2	OH
trpy	0.30	−0.07	0.51	0.15	0.99	0.51
	(0.25)	(0.08)	(0.51)	(0.35)	(0.76)	*b*
Me_3-tacn	0.35	0.02	0.53	*b*	1.03	0.54
	(0.31)	(0.10)	(0.55)	(0.38)	(0.79)	*b*

[a] Values in parentheses are redox potentials in H_2O/THF (9:1 v/v). [b] Not determined, insoluble.

(55) The pK_a value of $[Cr(OH_2)(3,5\text{-}Bu_2Cat)(trpy)]^{2+}$ produced by the base−acid treatments of **1s** were consistent with those of original **1c**.
(56) Photoirradiation was conducted under cutting off UV light (λ < 350 nm by Toshiba UV-35 filter).

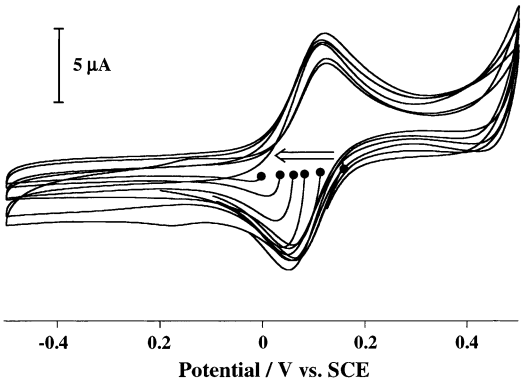

Figure 10. Change of the rest potential (E_{rest}) of the H_2O/THF (9:1 v/v) solution of $[Cr(OH)(3,5\text{-}Bu_2SQ)(Me_3\text{-}tacn)]^+$ at pH 11 for 15 h. CVs were measured about every 3 h and started from E_{rest}.

Moreover, photo-irradiation of the H_2O/THF solution of $[Cr(OH)(3,5\text{-}Bu_2SQ)(Me_3\text{-}tacn)]^+$ under illumination of a Xe lamp forced the same reduction to completion in 2 h.[56] Acidification of the solution from 11 to 4 caused the appearance of the $[Bu_2SQ]/[Bu_2Cat]$ redox couple at $E_{1/2} = 0.29$ V (vs SCE) of $[Cr(OH_2)(3,5\text{-}Bu_2Cat)(Me_3\text{-}tacn)]^{2+}$ (Table 5), because the rest potential of the solution was at a potential more negative than the redox potential of the $[Bu_2SQ]/[Bu_2Cat]$ couple. An investigation was undertaken to elucidate the mechanism for photochemical reduction of $[Cr(OH)(3,5\text{-}Bu_2SQ)(L)]^+$ in H_2O at pH 11.

Supporting Information Available: Figures (S1−S6) displaying fully labeled ORTEP drawings for **1c′**, **2**, **3**, **4**, **6**, and **7′** and one X-ray crystallographic file, in CIF format, for **1c′**, **2**, **3**, **4**, **6**, and **7′**. This material is available free of charge via Internet at http://pubs.acs.org.

IC020308M